Polym. Bull. (2013) 70:2873–2893
DOI 10.1007/s00289-013-0994-0

ORIGINAL PAPER

Origin of rheological behavior and surface/interfacial properties of some semi-alicyclic polyimides for biomedical applications

Silvia Ioan · Anca Filimon · Camelia Hulubei · Iuliana Stoica · Simona Dunca

Received: 15 March 2013 / Accepted: 1 June 2013 / Published online: 8 June 2013

Abstract High-performance alicyclic-containing polyimides for advanced applications, derived from 5-(2,5-dioxotetrahydrofurfuryl)-3-methyl-3-cyclohexene-1,2-dicarboxylic acid anhydride or bicyclo[2.2.2]oct-7-ene-2,3,5,6-tetracarboxylic dianhydride and two flexible aromatic diamines, were synthesized by a classical two-step polycondensation reaction and analyzed by rheological method. The results were discussed according to the chemical structure of polyimides and their different properties, such as flexibility, hydrophobicity and surface morphology. It has been showed that the obtained parameters, controlled by the interactions occurring in the polyimide systems, can be correlated with the adhesion/cohesion of blood components and plasma proteins. Thus, the results of the work of spreading proteins on the hydrophobic polyimide surfaces indicated that albumin is not absorbed preferentially, while fibrinogen is characterized by a higher degree of adhesion on the surfaces, and also that selective adsorption of plasma proteins modifies blood compatibility. In addition, these results and the ascertained antimicrobial activity of the studied polyimides contribute to the development of new applications in the bio-technical field.

Keywords Polyimide · Viscoelastic properties · Surface-interfacial properties · Biocompatibility · Antimicrobacterial

S. Ioan (✉) · A. Filimon · C. Hulubei · I. Stoica
"Petru Poni" Institute of Macromolecular Chemistry, Grigore Ghica Voda Alley, no 41A, 700487 Iasi, Romania
e-mail: ioan_silvia@yahoo.com; sioan@icmpp.ro

S. Dunca
Faculty of Biology, "Alexandru Ioan Cuza" University of Iasi, Bvd. Carol I, no 11, 700506 Iasi, Romania

Introduction

Polyimide (PI) materials exhibit exceptional thermal and mechanical properties, are easily processable as thin films from soluble precursors, and possess desirable dielectric properties, high optical transparency, low refractive index, and high glass transition temperature [1, 2]. For these reasons, they are among the most popular of all high-performance/high-temperature polymers, useful as membranes [3], composite matrices, films, fibers, foams [4], coatings and adhesives in microelectronics [5] and photoelectric industry [6]. In addition, polyimides are widely used in the microelectronic industry because of their low relative permittivity values. Since the signal propagation speed and wiring density in multichip packaging are dependent on relative permittivity [7], considerable effort has been extended in the last decade to design and synthesize new polyimides with lower relative permittivity. The greatest concentration of effort toward this end has involved modification of the chemical structure, for improving some properties, such as thermal stability, moisture absorption, optical properties, relative permittivity, and solubility [8]. To improve the solubility of polyimides, literature recommends incorporation of flexible linkages [9] and of aliphatic or alicyclic monomers [10], by the introduction of twisted [11] or unsymmetrical [12] structures, of bulky substituents [13], and also by copolymerization [14]. The combinations and types of aromatic and aliphatic monomers were selected according to the anticipated structure–property relations. Cycloaliphatic monomers impart rigidity to the polymer backbone, similar to that of aromatic diamines, but offer improvements in polymer transparency and dielectric constant, which is partially due to the reduced formation of charge transfer complexes [15]. Copolymerization of rigid plus flexible monomers (aromatic, cycloaliphatic, aliphatic) allows tailoring of the thermal and mechanical properties of polyimides for meeting specific processing and property requirements [16]. Recently, aliphatic and/or alicyclic polyimides have been acknowledged for their applications in optoelectronics (as substrates for displays) and nanoelectronics (as interinsulating layers), thanks to their higher transparency and lower relative permittivity, compared to those of aromatic polyimides. However, the thermal stability of aliphatic polyimides needs to be improved to the level of aromatic polyimides, to assure the reliability of the tested devices. Consequently, a good knowledge of their various properties is important for the management of various applications of polyimides.

In previous investigations [17, 18], we have synthesized different polyimide structures based on cycloaliphatic dianhydrides, such as homo- and co-polyimides. We have also studied some special properties of various polyimides-based blend systems, related to morphological and structural–rheological aspects [19, 20], blood compatibility [21], dielectric spectroscopy [22], or different novel approaches for patterning such type of polymers [23].

In the present study, the polyimides having a common monomer based on alicyclic, asymmetrical and flexible anhydride 5-(2,5-dioxotetrahydrofurfuryl)-

3-methyl-3-cyclohexene-1,2-dicarboxylic anhydride (DOCDA) or alicyclic, symmetrical and rigid dianhydride bicyclo[2.2.2]oct-7-ene-2,3,5,6- tetracarboxylic dianhydride (BOCA) and different aromatic diamines, 4,4′-oxydianiline (ODA) and 4-(4-((4-(4-aminophenoxy)phenyl)sulfonyl)phenoxy) (*p*-BAPS), respectively, were synthesized and rheologically investigated in *N*-methyl-2-pyrrolidone, at different concentrations and temperatures. Thus, utilization of a flexible and aliphatic dianhydride, DOCDA, or a rigid aromatic dianhydride, BOCA, as co-monomers, seems reasonable to reduce the polyimide chain–chain interaction and to disrupt the interaction among the aromatic moieties of ODA or *p*-BAPS diamines. On the other hand, as a consequence, a good knowledge on polyimide properties is important for their handling and formulation, and also for better understanding and controlling their different applications. For this reason, the rheological properties were correlated with the surface properties and control of the hydrophilic/hydrophobic balance. Such characteristics can affect the applications of polyimide materials as dielectric layers, because a higher water adsorption influences the reliability of the electrical circuit, and also as biomedical devices, a case in which the blood compatibility and antimicrobial activity studies here performed are of major medical importance.

Experimental details

Polymer synthesis

High-purity DOCDA (Merck 98 % purity), or BOCA (Aldrich >99 % purity) dianhydrides, and aromatic ODA (Aldrich 99 % purity), or *p*-BAPS (Aldrich 99.9 % purity) diamines, were used in the synthesis. Pure polyimides were prepared by a conventional two-stage thermal imidization process [8, 24]. In the former stage, four poly(amic acid)s (PAADOCDA-ODA, PAADOCDA-*p*-BAPS, PAABOCA-ODA and PAABOCA-*p*-BAPS) were prepared by addition of stoichiometric amounts of solid dianhydrides to the stirring solutions of the respective diamines, on keeping a 15 wt% solid content in a *N*-methyl-pyrrolidone (NMP) solvent. In the next stage, the thermal imidization reactions were carried out at temperature around 185 °C for 6 h. Scheme 1 presents the chemical structures of the resulting polyimides, poly(DOCDA-ODA), poly(DOCDA-*p*-BAPS), poly(BOCA-ODA), and poly(BOCA-*p*-BAPS), with the corresponding molecular weight of the structural units, M_0, and number average molecular weight, M_n.

Infrared spectroscopy

Fourier transform infrared spectroscopy (ATR-FTIR) was carried out to characterize polyimide films. Measurements were performed with a Nicolet-6700 ATR-FTIR spectrometer (Thermo Electron Corporation), on which the ATR spectra were recorded in the 500–4,000 cm^{-1} range [22].

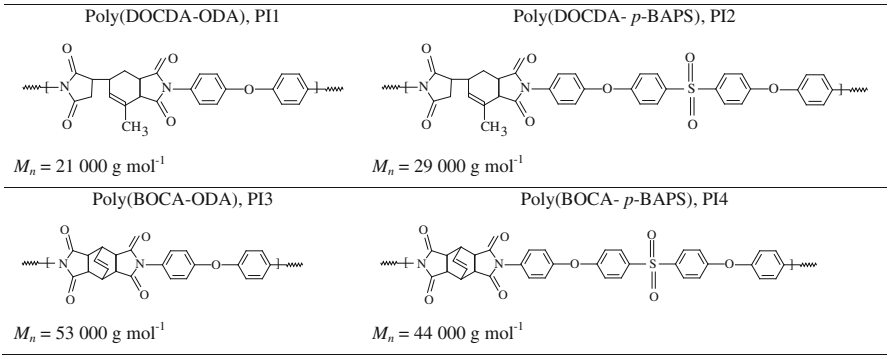

Scheme 1 General chemical structures of poly(DOCDA-ODA), poly(DOCDA-*p*-BAPS), poly(BOCA-ODA) and poly(BOCA-*p*-BAPS)

Proton NMR spectroscopy

^{1}H NMR spectra were obtained on a Bruker Avance DRX 400 MHz spectrometer for polyimide solutions in dimethylsulfoxide-d6 (DMSO-d6), using tetramethylsilane (TMS) as an internal standard.

Rheological investigations

The polyimide flow properties were determined on a Bohlin CS50 rheometer, manufactured by Malvern Instruments [20]. The measuring system presents a cone-plate geometry with a cone angle of 4° and a diameter of 40 mm. Shear viscosities were registered over the 0.5–1,000 s^{-1} shear rate domain, at several temperatures (25–40 °C). According to the amplitude sweep test realized at a frequency of 1 Hz, in the linear viscoelastic regime for shear stresses between 0.5 and 20 Pa, a shear stress of 10 Pa was selected for all samples. During oscillatory shear tests, frequency was varied between 0.1 and 60 Hz. For rheological measurements, a standard procedure for preparing polyimide solutions in NMP was applied. The values of concentration were around 24, 26 and 27 g dL^{-1} for all polymer solutions, and the rheological tests were obtained with an accuracy of ±5 %.

Contact angle measurements

For obtaining thin polyimide films, polymer solutions of 15 wt% in NMP were placed onto a glass substrate and first oven-preheated at 80 °C, followed by gradual heating at 100, 150, 200 and 250 °C, for 1 h at each temperature. The obtained thin films (around 40 μm) were stripped off the support by immersion in hot water, and then oven-dried at 105 °C.

The static contact angles of different test liquids on surface polymer films were measured using the sessile-drop method. Uniform drops of 2 μL test liquids [double-distilled water (W), methylene iodide (CH_2I_2), and 1-brom-naphthalene (1-Bn)] were deposited on the film surface and the contact angles were measured

after 30 s, with a video-based optical contact angle measuring device [25] equipped with a Hamilton syringe, in a temperature-controlled environmental chamber. The acid/base method (LW/AB) (Eqs. 1–3) [26] was utilized for calculating the surface tension parameters of poly(DOCDA-ODA), poly(DOCDA-*p*-BAPS), poly(BOCA-ODA), and poly(BOCA-*p*-BAPS); the surface properties of test liquids and biological materials [27–32] are presented in Table 1 and the contact angles measured between these liquids and the polyimide films, in Table 2.

$$1 + \cos\theta = \frac{2}{\gamma_{lv}}\left(\sqrt{\gamma_{sv}^{LW}\gamma_{lv}^{LW}} + \sqrt{\gamma_{sv}^{+}\gamma_{lv}^{-}} + \sqrt{\gamma_{sv}^{-}\gamma_{lv}^{+}}\right) \quad (1)$$

$$\gamma_{sv}^{AB} = 2\sqrt{\gamma_{sv}^{+}\gamma_{sv}^{-}} \quad (2)$$

$$\gamma_{sv}^{LW/AB} = \gamma_{sv}^{LW} + \gamma_{sv}^{AB} \quad (3)$$

where superscripts *LW/AB*, *AB* and *LW* refer to the total surface tension, polar component (calculated from the electron-donor, γ_{sv}^{-}, and electron-acceptor, γ_{sv}^{+}, interactions, according to Eq. 2), and disperse component, respectively.

Atomic force microscopy

Atomic force microscopy (AFM) was performed in air, at room temperature, using a Solver PRO-M Scanning Probe Microscope (NT-MDT, Zelenograd, Moscow, Russia) for both topographical and adhesion force measurements. The surface morphology of the polyimide films was studied in semi-contact mode, with a commercially available NSG03 rectangular-shaped silicon cantilever (length = 135 ± 5 μm, width = 30 ± 5 μm, thickness = 1–2 μm, probe tip radius = 10 nm). The scanning area was 3 × 3 μm^2. This particular type of cantilever, with a resonant frequency of 93 kHz, was also used for adhesion force studies, in contact mode. In this way, force curves can be obtained over the previously probed area, in

Table 1 Surface tension parameters (mN m^{-1}) of the test liquids used for contact angle measurements and of the biological materials

Material	γ_{lv}^{d}	γ_{lv}^{p}	γ_{lv}^{+}	γ_{lv}^{-}	γ_{lv}
Test liquid					
Water [27]	21.80	51.00	25.50	25.50	72.80
Methylene iodide [27]	50.80	0	0.72	0	50.80
1-Brom-naphthalene [28]	44.40	0	0	0	44.40
Biological material					
Red blood cell [28]	35.20	1.36	0.01	46.20	36.56
Platelet [28]	99.14	19.10	12.26	7.44	118.24
Blood [29, 30]	11.20	36.30	–	–	47.50
Fibrinogen [31]	37.60	3.89	0.10	38.00	41.50
Albumin [29, 30]	26.80	35.70	6.30	50.60	62.50
IgG [32]	34.00	17.30	1.50	49.60	51.30

Table 2 Contact angles of different test liquids on poly(DOCDA-ODA), poly(DOCDA-*p*-BAPS) and poly(BOCA-ODA), and poly(BOCA-*p*-BAPS) films

Sample	Contact angle (°)		
	W	CH_2I_2	1-Bn
Poly(DOCDA-ODA)	75	44	35
Poly(DOCDA-*p*-BAPS)	67	40	31
Poly(BOCA-ODA)	74	25	18
Poly(BOCA-*p*-BAPS)	68	21	14

semi-contact mode. In these measurements, deflections of the cantilever are recorded as probe tip approaches, contacts, and then withdrawn from the sample.

Antibacterial activity

The antibacterial properties of polyimide films were investigated by the agar diffusion method, their antibacterial efficiency being examined starting from the dimension of the inhibition zone generated in the presence of *Escherichia coli* ATCC 10536 (*E. coli*) and *Staphylococcus aureus* ATCC 6538 *(S. aureus)*. The bacteria were preincubated for 18 h at 37 °C. An agar plate with pH 7.2–7.4 at room temperature was uniformly inoculated with the test microorganism using a sterile cotton swab, and disinfected steel disks were placed on the agar surface. Circular polyimide films, 10 mm in diameter and 100 μm thick, were introduced in the disks. The plates were incubated at 37 °C for 24 h. The diameter of the inhibition zone depends both on the polymer present in the disk and on microorganism susceptibility.

Results and discussion

General properties of polyimides

According to Fig. 1, the FTIR spectra recorded for the studied samples confirm the structure of the synthesized polymers [22]. Thus, the characteristic imides absorption bands appear around 1,777–1,770 and 1,710–1,703 cm^{-1}, assigned to the C=O asymmetrical and symmetrical stretching vibrations of imide rings, and also around 1,384–1,382 and 784–769 cm^{-1}, assigned to C–N stretching and C–N bending, respectively, in imide groups. The aromatic structure is confirmed by the appearance of the 1,510 cm^{-1} peak, assigned to the =CH link from the benzene ring, whereas the absorptions bands at 2,927–2,925 and 3,068–3,035 cm^{-1} are assigned to the CH_2 vibration of the aliphatic units and to the C–H linkage of the aromatic rings, respectively. The ether bridge from ODA and *p*-BAPS diamine moieties is confirmed by the special bands at 1,239–1,232 cm^{-1}, while the $–SO_2$ asymmetrical and symmetrical stretching vibrations in the *p*-BAPS diamine

moieties, corresponding to poly(DOCDA-*p*-BAPS) and poly(BOCA-*p*-BAPS), appear at approximately 1,320 or 1,166 cm^{-1}.

In the same context, ^{1}H-NMR spectra confirm the structure of polyimides, as exemplified in Fig. 2 for poly(DOCDA-*p*-BAPS) and poly(BOCA-ODA).

The synergistic effect of polyimide structures on dynamic viscosity and viscoelasticity

Generally, according to Fig. 3, poly(DOCDA-ODA), poly(DOCDA-*p*-BAPS), poly(BOCA-ODA), and poly(BOCA-*p*-BAPS) having the common dianhydride DOCDA or BOCA exhibit a Newtonian behavior in a NMP solution, with a constant viscosity region over the entire shear rates range, at 25 °C. The same dependencies, characterized by constant dynamic viscosity over the entire shear rates, were obtained at all studied temperatures. On the other hand, the values of polyimides dynamic viscosity are expected to depend on their chain packing efficiency and intermolecular interactions, which in turn are influenced by rigidity degree of molecular backbone [33]. A previous paper [22] shows that synthesis of these polyimides follows control of chain flexibility and segment mobility by

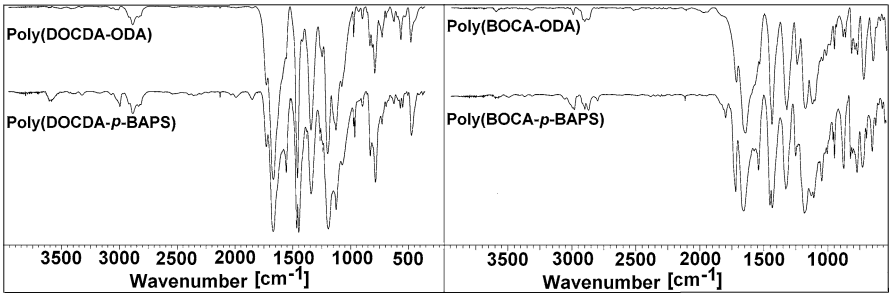

Fig. 1 ATR-FTIR of poly(DOCDA-ODA), poly(DOCDA-*p*-BAPS), poly(BOCA-ODA) and poly(BOCA-*p*-BAPS)

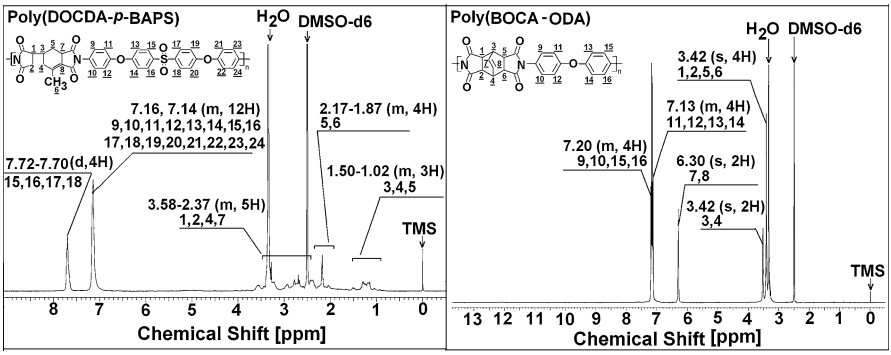

Fig. 2 ^{1}H NMR of poly(DOCDA-*p*-BAPS) and poly(BOCA-ODA)

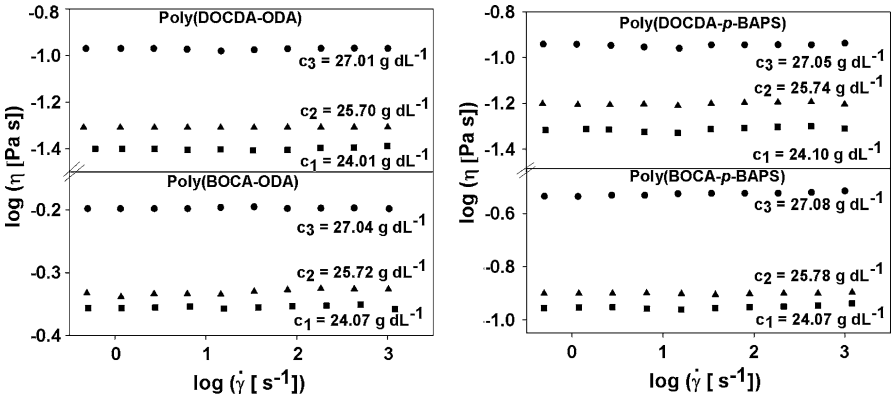

Fig. 3 Double logarithmic plot of viscosity versus shear rate for poly(DOCDA-ODA), poly(DOCDA-*p*-BAPS), poly(BOCA-ODA) and poly(BOCA-*p*-BAPS), in *N*-methyl-2-pyrrolidone at 25 °C and different concentrations

incorporation of alicyclic groups and flexible links, in order to reduce the strong intra- and intermolecular interactions that exist in conventional polyimides, by destruction of co-planarity and conjugation, reduction of symmetry and separation of the electronic chain segments. Therefore, utilization of an alicyclic dianhydride as a co-monomer, e.g., DOCDA or BOCA seems reasonable for reducing the polyimide chain–chain interaction and for disrupting the interactions among the aromatic moieties of ODA or *p*-BAPS diamines, thus influencing the rheological properties by increasing solubility. Moreover, the values obtained for dynamic viscosity are influenced by the low molecular density of these polyimides and by the presence of low polarizable groups—which reduce the probability of a $\pi \rightarrow \pi$ transition of the π-electronic system delocalized along the backbone chain. In addition, the molecular weights of the studied polymers with the same alicyclic dianhydride have close values (Scheme 1), so that their effect on dynamic viscosity was considered as minimum.

In agreement with these comments, Fig. 3 shows that the dynamic viscosity of poly(DOCDA-ODA)—with a flexible co-monomer DOCDA, in the presence of ether linkages from ODA diamine (which distinctly disturbs the close packing of the polymer chains, increasing the free volume and reducing the interchain electronic interactions [22])—is slightly lower than the dynamic viscosity of poly(DOCDA-*p*-BAPS) with the same dianhydride, but in the presence of ether and sulfone linkages (which determines a decrease of the free volume, as due to the competition between the increase of interchain interactions and the steric effects, with opposite contributions [22, 34], and increases the electronic conjugation chains from *p*-BAPS diamine). Thus, at 25 °C dynamic viscosity is modified in the ranges of 0.03–0.10 Pa s, and of 0.04–0.12 Pa s, for poly(DOCDA-ODA) and poly(DOCDA-*p*-BAPS), respectively, when the concentration increases over the 24–27 g dL^{-1} domain.

Secondly, the lower values obtained for poly(BOCA-*p*-BAPS), compared with poly(BOCA-ODA), could be the result of a synergetic steric hindrance effect induced by the bicyclic non-coplanar group of BOCA moieties and of the $–SO_2$

group from diamine. This cumulative effect increases the free volume and decreases the number of polarizable groups per volume unit, lowering polarization in comparison with DOCDA dianhydride [22]. In this context, according to Fig. 3, dynamic viscosity take values in the range of 0.43–0.63 and 0.11–0.30 Pa s for poly(BOCA-ODA) and poly(BOCA-*p*-BAPS), respectively, when concentration increases over the 24–27 g dL^{-1} domain.

On the other hand, according to the thermodynamic of polymer solutions, the dynamic viscosity values of polyimides with higher rigidity and molecular weight, due to BOCA dianhydride moieties, are superior to those containing DOCDA dianhydride moieties.

The Newtonian flow behavior is also confirmed by the values obtained for the flow ($n \cong 1$) and consistency indices (K), from the dependence of shear stress, σ, on shear rate, described by Eq. 6 (Ostwald–de Waele relationship).

$$\sigma = K\dot{\gamma}^n \tag{4}$$

According to Table 3, the results for PI samples in NMP reveal that the flow indices are equal to unity, confirming the Newtonian behavior for all concentrations, while increase of shear stress with concentration and polyimide rigidity (i.e., for those containing BOCA moieties) generates higher values of consistency indices in the NMP solutions.

The interactions among chain segments in the presence of NMP induce modifications of dynamic viscosity with temperature, as reflected in the values of activation energy (Table 3) expressed by Arrhenius equation:

$$\ln \eta = \ln \eta_0 + \frac{E_a}{RT} \tag{5}$$

where $\eta_0 \propto e^{-\Delta S/R}$ [35] represents a pre-exponential constant, ΔS is the flow activation entropy, R is the universal gas constant and T is absolute temperature.

Table 3 Flow behavior index, consistency index and activation energy for polyimides at different concentrations and 25 °C

Polyimide	c (g dL^{-1})	n	K	E_a (kJ mol^{-1})
PI1	24.01	1.05	0.03	22.46
	25.71	1.04	0.07	24.29
	27.01	1.01	0.09	24.98
PI2	24.10	1.04	0.04	22.26
	25.74	0.99	0.07	22.58
	27.05	1.05	0.08	24.72
PI3	24.07	1.02	0.41	22.75
	25.72	1.00	0.46	24.96
	27.04	1.01	0.60	25.92
PI4	24.07	1.05	0.09	22.35
	25.78	1.00	0.13	24.76
	27.08	1.01	0.29	25.90

A lower value of E_a implies a lower energy barrier for the movement of an element in the fluid, and corresponds to a higher flexibility of the polymer chain. In the case of involved polyimides solutions, flexibility increases in the order: poly(DOCDA-ODA) < poly(DOCDA-*p*-BAPS), poly(BOCA-ODA) < poly(BOCA-*p*-BAPS), and causes a decrease in activation energy, as shown in Table 3. On the other hand, the positive values of activation energy for all polyimides are generated by the positive contribution of disengagement, which becomes preponderant, compared with the negative contribution from the associated formations, which shows that, from a thermodynamic point of view, NMP is a good solvent.

The effect of the chemical structure of polyimides on the viscoelastic properties, reflected in the mobility of the segments from the shear field, is quantified by storage, G', and loss, G'', moduli. Prior to the experimental measurements, a suitable strain amplitude test was performed, involving measurement of the strain dependence of moduli, to ensure the linearity of viscoelasticity. Also, a stress sweep experiment was performed to establish sample's resistance to deformation at a constant frequency of 1 Hz. Figure 4 illustrates the variation of the storage and loss modulus, respectively, versus strain amplitude and shear stress for all polyimides at a concentration around 24 g dL^{-1}. G' and G'' are constant and G' is lower than G'', showing viscoelastic fluid properties over the whole range of deformation. In this context, a 10 Pa shear stress value was selected for the viscoelasticity measurements plotted in Fig. 5, as a function of frequency.

Over the studied frequency range, the storage moduli, loss moduli, and the corresponding frequency of transition from the viscous to the elastic flow, when $G' = G''$, appear as strongly related to the chemical structure of polyimides,

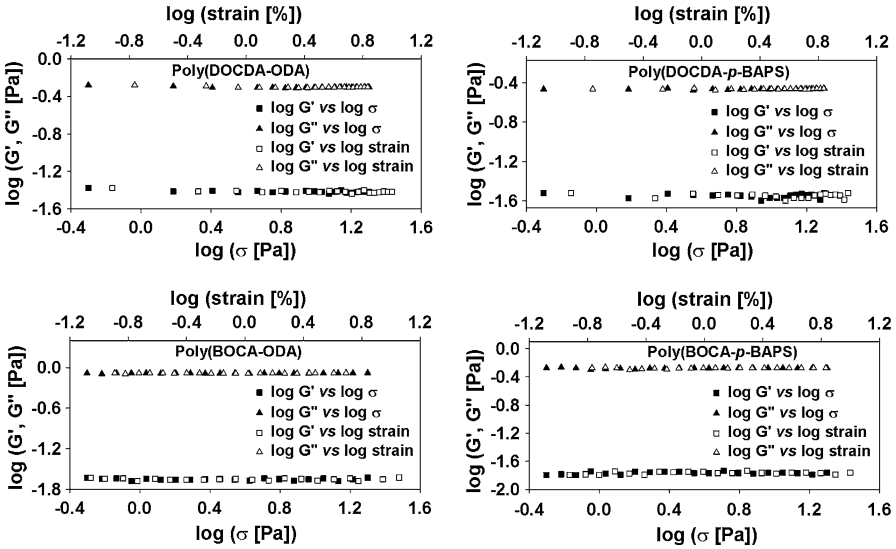

Fig. 4 Log-log of storage and loss moduli versus shear stress and strain amplitude, for poly(DOCDA-ODA), poly(DOCDA-*p*-BAPS), poly(BOCA-ODA) and poly(BOCA-*p*-BAPS) at about 10 g dL^{-1} concentration in *N*-methyl-2-pyrrolidone, and 25 °C

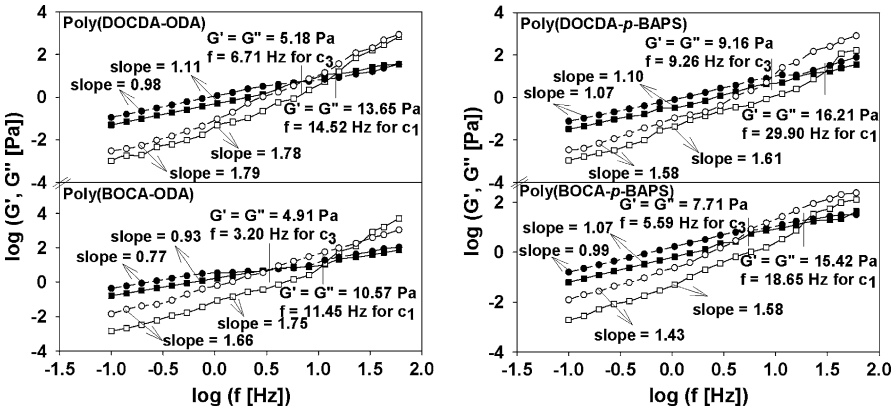

Fig. 5 Double logarithmic plot of storage and loss moduli as a function of frequency for poly(DOCDA-ODA), poly(DOCDA-*p*-BAPS), poly(BOCA-ODA) and poly(BOCA-*p*-BAPS) solutions in *N*-methyl-2-pyrrolidone at two concentrations, $c_1 \cong 24$ and $c_3 \cong 27$ g dL^{-1}, and 25 °C

reflecting the influence of flexibility. Typically, at lower frequency, higher values of G'', lower values of G' and higher values of the frequencies for which $G' = G''$ were obtained when the flexibility of polyimide with the same dianhydride is enhanced by the presence of *p*-BAPS diamine. At higher values of frequency, G' becomes higher than G'', and the frequency corresponding to their overlapping increases with decreasing concentration. The storage and loss moduli also exhibit the power-law dependence on frequency, where exponents around 2 and 1, respectively, are characteristic to viscoelastic fluids.

The magnitude of $\tan\delta = G''/G'$ indicates the relative amount of energy dissipated by the material during cyclic stress in oscillatory testing. The favorable interactions among chains decrease the free volume, and consequently, its behavior becomes more elastic, and the intensity of $\tan\delta$ decreases. According to Fig. 6, at lower frequency (in the viscous domain) polyimides take constant values of phase angles, δ. At the same time, polyimides based on BOCA dianhydride have higher values of $\tan\delta$ than those based on DOCDA dianhydride, but containing the same diamine, whereas polyimides derived from *p*-BAPS diamine have lower values than those derived from ODA diamine, but the same dianhydride. Therefore, the factors that contribute to these interactions may include the similarities of the main chain structures of the polymers with a common monomer, diamine or dianhydride.

Surface and interfacial properties of semi-alicyclic polyimides

One can mention that for all studied polyimides, the rheological properties are influenced by the high hydrophobic characteristics; the low polarization arising from the dipole orientation and trapped charge carriers generates electron–donor interactions higher than the electron–acceptor ones, according to Table 4. In this context, for each pair of polyimide having the same dianhydride segment, the presence of *p*-BAPS diamine leads to a higher polar component, γ_{sv}^{AB}, of surface

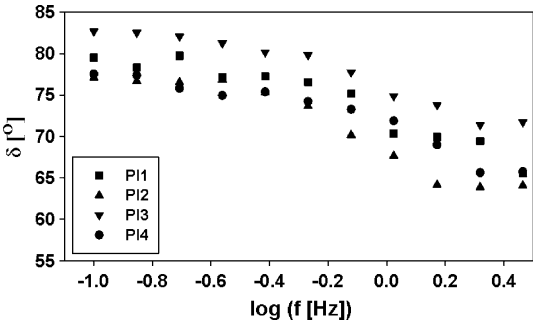

Fig. 6 Phase angle versus oscillation frequency for poly(DOCDA-ODA), poly(DOCDA-*p*-BAPS, poly(BOCA-ODA), and poly(BOCA-*p*-BAPS) solutions in NMP at 24 g dL^{-1} concentration, and 25 °C

Table 4 Surface tension parameters (mN m^{-1}) for poly(DOCDA-ODA) (PI1), poly(DOCDA-*p*-BAPS) (PI2), poly(BOCA-ODA) (PI3) and poly(BOCA-*p*-BAPS) (PI4) films prepared from solutions in NMP, according to the acid/base method (LW/AB), and surface free energy (ΔG_w) (mJ m^{-2})

Sample	LW/AB method					
	γ_{sv}^{LW}	γ_{sv}^{+}	γ_{sv}^{-}	γ_{sv}^{AB}	$\gamma_{sv}^{LW/AB}$	ΔG_w
PI1	36.70	0.70	7.09	4.46	41.16	-91.7
PI2	38.58	1.40	10.80	7.77	46.35	-101.3
PI3	42.58	0.30	7.77	3.07	45.65	-92.9
PI4	43.43	0.85	9.55	5.68	49.11	-100.1

tension, $\gamma_{sv}^{LW/AB}$, compared with the presence of ODA diamine. Increase of the free volume and reduction of the interchain electronic interactions are caused by the presence of ODA moieties, while decrease of the free volume and increase of electronic conjugation are associated with the *p*-BAPS moieties and implicitly, with the presence of sulfone groups.

In addition, for the same diamine, the γ_{sv}^{AB} value for BOCA-based polyimides is lower than those of the related polyimides with DOCDA dianhydride moieties. As mentioned in literature [11, 36], different properties of polyimides, such as interchain distance and fractional free volume, are dependent on the microstructural characteristics. Thus, previous wide-angle X-ray diffraction experiments (WAXD) [22] showed that the DOCDA-based polyimide films present no crystallinity, due to their non-symmetrical and flexible structure, and that these features are responsible for the irregularity and non-linearity of the polymer chains, disturbing chain packing. Moreover, ODA or *p*-BAPS contributes with additional flexibility, leading to the decrease of chain packing regularity. Such cumulative effects determine the amorphous character of these polyimides. In the case of BOCA-based polyimide films, WAXD experiments show some regularity of the intermolecular packing, combined with an amorphous halo. Thus, BOCA moieties exhibit a non-coplanar configuration, due to the geometrical constraints of the macromolecular chains. Consequently, the intersegmental distance and the free volume fraction are 5.06 Å and 10.21 % for poly(BOCA-ODA), and 5.43 Å and 10.86 % for poly(BOCA-*p*-BAPS), respectively.

On the other hand, the effect of the chemical structure on the surface and interfacial properties, evaluated by Eqs. 6–8, evidences a high hydrophobicity of polyimides, characterized by a surface free energy (ΔG_w) higher than -113 mJ m^{-2} [22, 27] (Table 4), and also negative values of the interfacial free energy (ΔG_{sls}, Fig. 7), denoting attraction between the two polyimide surfaces, *s*, immersed in water, *l*.

$$\Delta G_w = -\gamma_{lv}(1 + \cos\theta_{\text{water}}) \tag{6}$$

$$\Delta G_{sls} = -2\gamma_{sl} \tag{7}$$

$$\gamma_{sl} = \left(\sqrt{\gamma_{lv}^{p}} - \sqrt{\gamma_{sv}^{AB}}\right)^2 + \left(\sqrt{\gamma_{lv}^{d}} - \sqrt{\gamma_{sv}^{LW}}\right)^2 \tag{8}$$

where γ_{sl} indicates the solid–liquid interfacial tension.

In the same context, the work of spreading of water over the polyimide surfaces, W_s, takes negative values (Fig. 8). According to Eq. 9, it is estimated that the work of water adhesion, W_a, is low compared with the work of cohesion, W_c, a behavior caused by the hydrophobic characteristics of polyimides.

$$W_s = W_a - W_c = 2[(\gamma_{sv}^{LW}\gamma_{lv}^{d})^{0.5} + (\gamma_{sv}^{+}\gamma_{lv}^{-})^{0.5} + (\gamma_{sv}^{-}\gamma_{lv}^{+})^{0.5}] - 2\gamma_{lv} \tag{9}$$

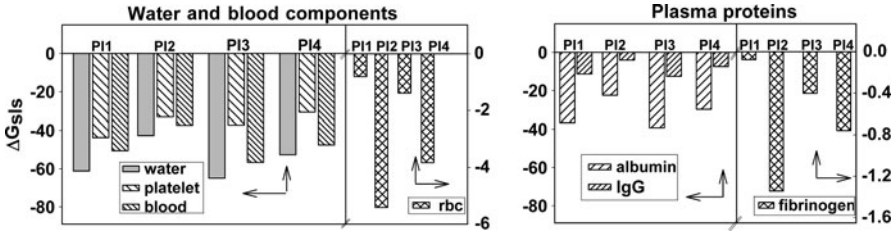

Fig. 7 Interfacial free energy, ΔG_{sls}, between two particles of polyimides in water, blood components and plasma proteins phases

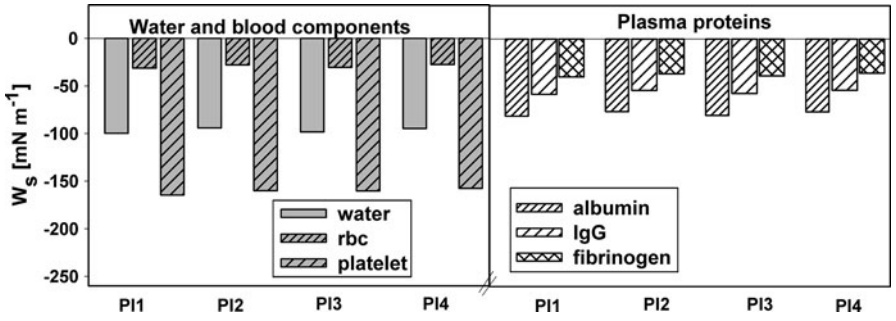

Fig. 8 Work of spreading of water, blood components and plasma proteins over the surface of polyimides

AFM studies of semi-alicyclic polyimides

The effect of surface morphology of polyimides on hydrophobicity was investigated by AFM in semi-contact mode. Three-dimensional (3D) topographical AFM images (Fig. 9a–d) revealed that all investigated polyimides formed films with uniform and smooth surfaces. This is also highlighted by the low values of the root mean square roughness parameter, S_q, (<1 nm), as shown in Table 5. However, different morphologies can be observed by means of the cross-section plots (Fig. 9a′–d′) taken along the lines in 3D images, generated by different flexible aromatic diamines introduced in the polyimides backbones. Height profile analysis emphasized the morphological features of nanometer-sized granules. In addition, for polyimides containing ODA diamine, the slightly higher values of average height (H_a) and S_q parameter, are associated with a higher degree of disorder in grain structure distribution, compared with polyimides containing *p*-BAPS diamine (Table 5).

Because the polymer film topography showed no major differences among the samples, the local surface properties were investigated by the AFM technique. Force–distance spectroscopy DFL (height) was used to measure the adhesion forces between polyimides samples' surface and the silicon cantilever. In contact mode, the adhesion forces have a significant effect on the cantilever during its withdrawal

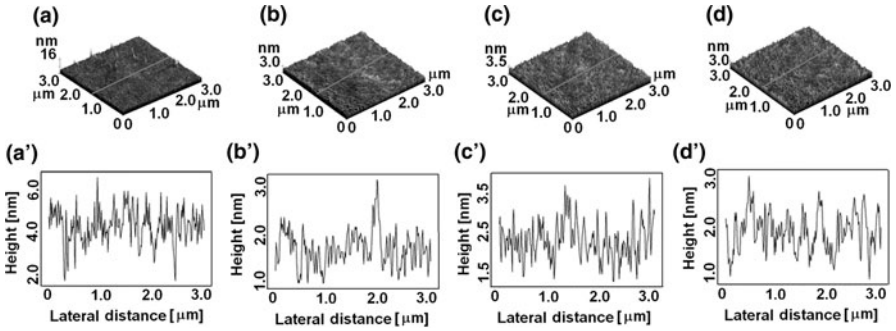

Fig. 9 3D AFM images (**a**–**d**) and corresponding profiles (**a′**–**d′**) for poly(DOCDA-ODA), poly(DOCDA-*p*-BAPS), poly(BOCA-ODA) and poly(BOCA-*p*-BAPS), respectively

Table 5 Surface roughness parameters [average height (H_a, nm), and root mean square roughness (S_q, nm) and force–distance spectroscopy DFL (height) measurements, number of curves and mean adhesion force (F_{adh}, nN)] obtained from AFM investigation for 3 × 3 μm^2 scan area

Sample	Surface roughness parameters		DFL (height) measurements	
	H_a	S_q	Number of curves	F_{adh}
Poly(DOCDA-ODA)	4.3	0.85	10	28.3 ± 3.9
Poly(DOCDA-*p*-BAPS)	1.7	0.36	10	46.8 ± 2.4
Poly(BOCA-ODA)	2.3	0.52	10	57.9 ± 5.2
Poly(BOCA-*p*-BAPS)	1.9	0.41	10	46.9 ± 6.5

from the sample. These forces cause deflection of the cantilever before it interrupts the contact with the surface. With the z-scanner length being reduced, the DFL (normal deflection distribution of the cantilever) first falls below its value, observed well away from the surface, and then abruptly reaches the free-state value, thus forming a specific dip. The adhesion force was calculated as a linear function of the probe displacement relative to the sample surface along to the *Z*-axis, according to Hooke's law, expressed by Eq. 10:

$$F = -k\Delta x \tag{10}$$

where k is cantilever stiffness, and Δx is deflection of the cantilever in rapport with polyimide film surface.

Cantilever's normal spring constant, k, of 1.97 N m^{-1}, was determined by Sader's method, using data on the resonance peak of 93 kHz and the planar dimensions of the cantilever [37, 38]. Figure 10a, b, c, and d shows the representative approach and retraction curves performed on poly(DOCDA-ODA), poly(DOCDA-*p*-BAPS), poly(BOCA-ODA) and poly(BOCA-*p*-BAPS), respectively. The inset plots depict the detailed retraction curves. For every experiment, the average value of the adhesion force was determined from the 10 retraction DFL (height) curves, according to Table 5.

Analysis of the occurrence of the retraction curves from Fig. 10 evidences differences between the surface properties of the polyimide films. Generally, assuming that the cleaned and dried silica surface of the cantilever is hydrophobic, the interactions between a hydrophobic tip and a hydrophobic substrate will be higher than those between a hydrophobic tip and a hydrophilic substrate, respectively [39]. Therefore, the higher value of the mean adhesion force obtained for poly(BOCA-ODA) (Fig. 10c) can be explained by its more hydrophobic nature,

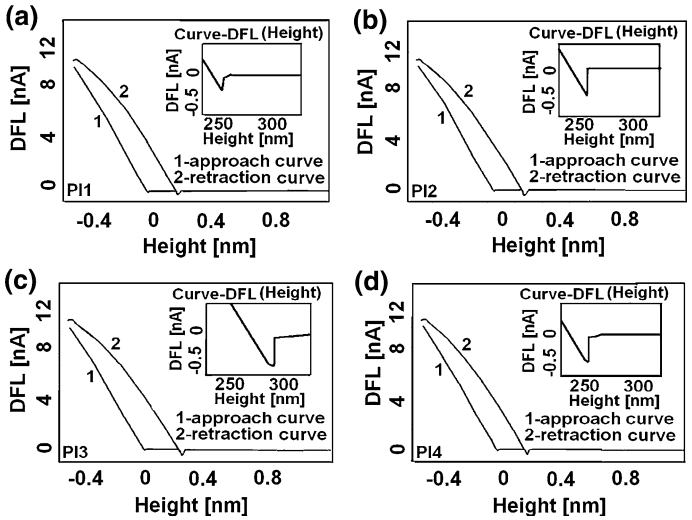

Fig. 10 Force–distance spectroscopy DFL (*height*) performed on: **a** poly(DOCDA-ODA), **b** poly(DOCDA-*p*-BAPS), **c** poly(BOCA-ODA) and **d** poly(BOCA-*p*-BAPS)

while the lower adhesion force is recorded for the poly(DOCDA-ODA) sample (Fig. 10a; Table 5). The close values of the mean adhesion force obtained for poly(BOCA-*p*-BAPS) (Fig. 10d) and poly(DOCDA-*p*-BAPS) (Fig. 10b) indicate similar surface wetting characteristics, according to the results on surface properties.

Identification of semi-alicyclic polyimides compatibility with blood components and antimicrobial activity

Surface analysis of polyimides was performed also for obtaining better understanding the interfacial chemistry of adhesion not only with water, but also with blood components and plasma proteins. The interactions between blood and a polymer surface depend on blood composition, blood flow and the physicochemical properties of the polymer surface, such as crystallinity, hydrophobicity/hydrophilicity, or the toxicological and electrical properties [40–42]. On the other hand, bio-incompatible polymers are largely used for devices in contact with blood, in conditions in which blood coagulation is regulated by anticoagulants. In this context, a previous paper [22] shows that these semi-alicyclic polyimides, with a suitable macromolecular design, poly(DOCDA-ODA), poly(DOCDA-*p*-BAPS), poly(BOCA-ODA) and poly(DOCDA-*p*-BAPS), may potentially offer important advantages for bio-microelectronic applications, due to their low dielectric constant values, in the 2.73–3.33 range at 25 °C, and to the electrical conductivity based on energy bandgap representation. Blood compatibility is generated by the modality in which the polyimide surface interacts with blood constituents, such as the red blood cells (rbc) and platelets (p), and also with plasma proteins, such as albumin, immunoglobulin G (IgG), and fibrinogen. In this context, the solid (polyimides)–liquid (blood components and plasma proteins) interfacial tensions, γ_{sl}, and the interfacial free energy between two polyimide particles in blood phase, ΔG_{sls} (Eqs. 7 and 8), show that an attraction occurs between the two polyimide surfaces, *s*, immersed in various components found in blood (Fig. 7). In addition, the work of spreading of blood components ($W_{s,rbc}$, $W_{s,p}$), and plasma proteins ($W_{s,albumin}$, $W_{s,IgG}$, and $W_{s,fibrinogen}$), over the polyimide surfaces was evaluated with Eq. 9, using the surface energy parameters (γ_{lv}, γ_{lv}^{d}, γ_{lv}^{+}, γ_{lv}^{-}) given in Table 1 for biological materials [28, 32]. According to the negative values of the interfacial free energy of the studied polyimides, the work of spreading of different blood components (Fig. 8) takes negative values, suggesting a lower work of adhesion, compared with that of cohesion. Particularly, the results show that exposure of platelets to poly(DOCDA-ODA), poly(DOCDA-*p*-BAPS), poly(BOCA-ODA) and poly(DOCDA-*p*-BAPS) films increases their cohesion and also that a good hydrophobicity is correlated with a lower cohesion of the red blood cells. Moreover, exposure of plasma proteins to polyimide films generates high albumin cohesion, followed by lower values of IgG and fibrinogen cohesion.

Generally, considering that blood is exposed to a biomaterial surface, cell adhesion decides the life of the implanted biomaterials. Cellular adhesion to the biomaterial surfaces can activate coagulation and immunological cascade, having a direct impact on the thrombogenicity and immunogenicity of a biomaterial, thus

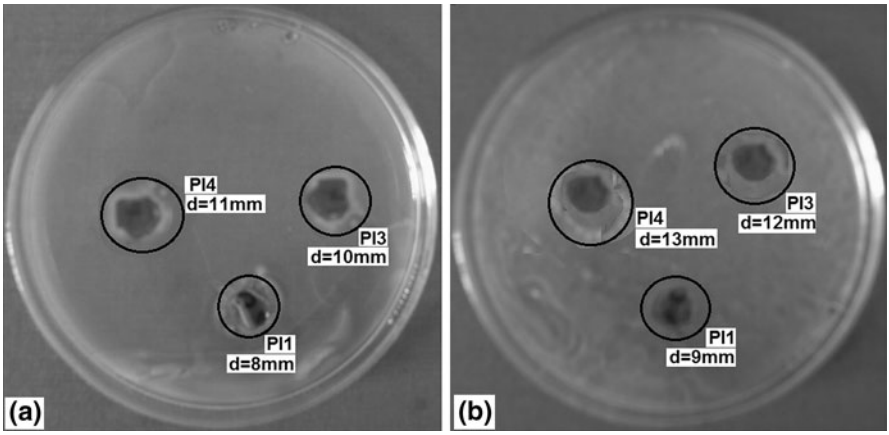

Fig. 11 Influence of poly(DOCDA-ODA), poly(BOCA-ODA) and poly(BOCA-*p*-BAPS) on growth of *E. coli* (**a**) and *S. aureus* (**b**) bacteria, expressed by the inhibition zone diameter, *d*

influencing its blood compatibility [21, 42, 43]. Consequently, blood compatibility implies prevention of platelet adhesion and deactivation of the intrinsic coagulation system, generated by the competitive blood protein adsorption on the polymer surface. Adhesion of platelets is promoted by the adsorbed fibrinogen and gamma globulin, whereas the adsorbed albumin inhibits platelet adhesion. It is also demonstrated that albumin adheres to a hydrophilic surface rather than to a hydrophobic one, whereas fibrinogen adheres to a hydrophobic surface [44, 45]. Moreover, literature shows that adhesion of the red blood cells onto a surface requires knowledge of the interactions with the vascular components [21, 46]. Thus, endothelial glycocalyx, along with the mucopolysaccharides adsorbed onto the endothelial surface of the vascular endothelium, reject the clotting factors and platelets, known as playing a significant role in thrombus formation. In this context, such results can be applied for the encapsulation of some implantable biosensors to form a biocompatible interface between the probe and the brain tissue [21, 47, 48], being equally useful for evaluating bacterial adhesion to the polymer surface, in the study of some possible infections induced by implanted devices.

The antibacterial activity of polyimide films was investigated against *E. coli* and *S. aureus*. The studied polyimide interferes with the bacterial metabolism by electrostatic stacking at the cell surface of bacteria. In this context, the specific compositions of the cell wall of Gram-negative (*E. coli*) and Gram-positive (*S. aureus*) bacteria induce different antimicrobial activity. The component of Gram-positive bacteria cell walls is peptidoglycan, which confers the hydrophobic character of *S. aureus*, while the major constituent of Gram-negative bacteria cell walls is peptidoglycan, together with other membranes, such as lipopolysaccharides and proteins, assuring the hydrophilic character of *E. coli* [49].

Figure 11 shows the slightly different inhibiting effects of polyimides with hydrophobic characteristics on the tested *E. coli* and *S. aureus*. It is found that *S. aureus* is more sensitive than *E. coli* to the polyimide with hydrophobic surface,

while the polyimides with BOCA dianhydride inhibit the bacteria more than polyimides with DOCDA dianhydride.

Moreover, literature shows that BOCA di anhydride is especially interesting, due to its molecular architecture which can serve in the design of therapeutic agents [50].

It can be concluded that the exact mechanism of the inhibiting effect of these microorganisms is complex, considering that, besides the wall compositions of these bacteria and surface properties of polyimides, other types of interactions also occur, e.g., van der Waals and electrostatic interactions. Thus, the obtained results indicate that adhesion of *E. coli* and *S. aureus* to polyimide surfaces is mediated mainly by specific interactions, rather than by hydrophobic interactions.

Conclusions

Partially aliphatic polyimides with different flexibilities, poly(DOCDA-ODA), poly(DOCDA-*p*-BAPS), poly(BOCA-ODA) and poly(BOCA-*p*-BAPS) obtained by a polycondensation reaction between DOCDA and BOCA dianhydrides and the flexible aromatic diamines ODA or *p*-BAPS, were studied as to their dynamic viscosity, viscoelasticity, surface properties and blood compatibility.

The investigations indicate that, for the same diamine, the non-coplanar configuration of BOCA moieties induced geometrical constrains in the macromolecular chains and, implicitly, determines a high rigidity of these polyimides that explains their higher dynamic viscosity, compared with polyimides based on DOCDA dianhydride. The presence of ODA diamine with ether linkages in polyimides, which disturbs close packing of the polymer chains and increases the free volume, causes a decrease in dynamic viscosity compared with *p*-BAPS diamine with ether and sulfone linkages—where the competition between the increase of interchain interactions and the steric effects reduces the free volume. In this context, the constant values of dynamic viscosity at different shear rates, and the values obtained for the flow behavior and consistency indices from the Ostwald–de Waele model, indicate a Newtonian behavior for all studied polyimides. Moreover, a lower value of activation energy corresponds to a higher flexibility of the polyimide chains, which increases in the following order: poly(DOCDA-ODA) < poly(DOCDA-*p*-BAPS), poly(BOCA-ODA) < poly(BOCA-*p*-BAPS), whereas the positive values of the activation energy assume a positive contribution of disengagement, which becomes preponderant, compared with the negative contribution resulting from the association phenomena.

The effect of the chemical structure of polyimides on the viscoelastic properties is reflected in the higher values of G'' the lower values of G' and the higher values of the crossover point delimiting the viscous flow from the elastic one, for a higher flexibility of polyimides.

On the other hand, the effect of chemical structure on the surface and interfacial properties evidences a lower hydrophilicity of polyimides, characterized by a surface free energy higher than -113 mJ m^{-2}, and also negative values of interfacial free energy, denoting attraction between the two polyimide surfaces

immersed in water. In addition, the AFM studies reveal some differences among the surface properties of the polyimide films. Interactions between the hydrophobic cantilever and polymer hydrophobic substrate are reflected in a higher mean adhesion force.

Moreover, the results show that surface hydrophobicity controls the compatibility with blood components and plasma proteins. Thus, the proteins spread on the hydrophobic polyimide surfaces indicated that albumin is not preferentially absorbed, while fibrinogen is characterized by a higher degree of adhesion on the surfaces, and also that the selective adsorption of plasma proteins modifies blood compatibility. Apart from that, certain inhibitory effects of polyimides on the growth of *E. coli* and *S. aureus* bacteria have observed. These properties are useful in investigations on specific biomedical applications, including evaluation of bacterial adhesion to the surfaces, and utilization of modified polyimides as semipermeable membranes.

Acknowledgments The Romanian National Authority for Scientific Research (CNCS, UEFISCDI; Project PN-II-ID-PCE-2011-3-0937, No. 302/5.10.2011; 2013 phase) is contract grant sponsor.

References

1. Ando S (2004) Optical properties of fluorinated polyimides and their applications to optical components and waveguide circuits. J Photopolym Sci Technol 17:219–232
2. Maier G (2001) Low dielectric constant polymers for microelectronics. Prog Polym Sci 26:3–65
3. Gonzalo B, Vilas JL, Breczewski T, Perez-Jubindo MA, De La Fuente MR, Rodriguez M, Leon LM (2009) Synthesis, characterization, and thermal properties of piezoelectric polyimides. J Polym Sci Part A Polym Chem 47:722–730
4. Wang S, Zhou HW, Dang GD, Chen C (2009) Synthesis and characterization of thermally stable, high-modulus polyimides containing benzimidazole moieties. J Polym Sci Part A Polym Chem 47:2024–2031
5. Zhang QX, Naito K, Tanaka Y, Kagawa Y (2008) Grafting polyimides from nanodiamonds. Macromolecules 41:536–538
6. Chang CM, Chang CC (2008) Preparation and characterization of polyimide–nanogold nanocomposites from 3-mercaptopropyl-trimethoxysilane encapsulated gold nanoparticles. Polym Degrad Stabil 93:109–116
7. Hougham G, Tesoro G, Viehbeck A, Chapple-Sokolg JD (1994) Polarization effects of fluorine on the relative permittivity in polyimides. Macromolecules 27:5964–5971
8. Myung BY, Kim JS, Kim JJ, Yoon TH (2003) Synthesis and characterization of novel polyimides with 2,2-bis[4(4-aminophenoxy)phenyl]phthalein-3′,5′-bis(trifluoromethyl)anilide. J Polym Sci Part A Polym Chem 41:3361–3374
9. Yang CP, Hsiao SH, Wu KL (2003) Organosoluble and light-colored fluorinated polyimides derived from 2,3-bis(4-amino-2-trifluoromethylphenoxy)naphthalene and aromatic dianhydrides. Polymer 44:7067–7078
10. Yang CP, Su YY, Hsiao FZ (2004) Synthesis and properties of organosoluble polyimides based on 1,1-bis[4-(4-amino-2-trifluoromethylphenoxy)phenyl]cyclohexane. Polymer 45:7529–7538
11. Eichstadt AE, Ward TC, Bagwell MD, Farr IV, Dunson DL, McGrath JE (2002) Synthesis and characterization of amorphous partially aliphatic polyimide copolymers based on bisphenol-A dianhydride. Macromolecules 35:7561–7568
12. Chou CH, Reddy DS, Shu CF (2002) Synthesis and characterization of spirobifluorene-based polyimides. J Polym Sci Part A Polym Chem 40:3615–3621
13. Chung IS, Kim SY (2000) Soluble polyimides from unsymmetrical diamine with trifluoromethyl pendent group. Macromolecules 33:3190–3193

14. Hwang HJ, Li CH, Wang CS (2006) Dielectric and thermal properties of dicyclopentadiene containing bismaleimide and cyanate ester. Part IV. Polymer 47:1291–1299
15. Chern YT, Shiue HC (1997) Low dielectric constants of soluble polyimides derived from the novel 4,9-bis[4-(4-aminophenoxy)phenyl]diamantine. Macromolecules 30:5766–5772
16. Kreuz JA, Hsiao BS, Renner CA, Goff DL (1995) Crystalline homopolyimides and copolyimides derived from 3,3′,4,4′-biphenyltetracarboxylic dianhydride/1,3-bis(4-aminophenoxy)benzene/1,12-dodecanediamine. 1. Materials, preparation, and characterization. Macromolecules 28:6926–6930
17. Hulubei C, Popovici D (2011) Novel polyimides containing alicyclic units. Synthesis and characterization. Rev Roum Chim 56:209–215
18. Popovici D, Hulubei C, Cozan V, Lisa G, Bruma M (2012) Polyimides containing cycloaliphatic segments for low dielectric material. High Perform Polym 24:194–199
19. Cosutchi AI, Hulubei C, Stoica I, Ioan S (2010) Morphological and structural–rheological relationship in epiclon-based polyimide/hydroxypropylcellulose blend systems. J Polym Res 17:541–550
20. Cosutchi AI, Nica SL, Hulubei C, Homocianu M, Ioan S (2012) Effects of the aliphatic/aromatic structure on the miscibility, thermal, optical, and rheological properties of some polyimide blends. Polym Eng Sci 52:1429–1439
21. Nica SL, Hulubei C, Stoica I, Ioanid GE, Ioan S (2013) Surface properties and blood compatibility of some aliphatic/aromatic polyimide blends. Polym Eng Sci 53:263–272
22. Ioan S, Hulubei C, Popovici D, Musteata VE (2012) Origin of dielectric response and conductivity of some alicyclic polyimides. Polym Eng Sci. doi:10.1002/pen.23409
23. Cosutchi AI, Hulubei C, Stoica I, Ioan S (2011) A new approach for patterning epiclon-based polyimide precursor films using a lyotropic liquid crystal template. J Polym Res 18:2389–2402
24. Hamciuc E, Lungu R, Hulubei C, Bruma M (2006) New poly(imide-ether-amide)s based on epiclon. J Macromol Sci Part A Pure Appl Chem 43:247–258
25. Ioanid EG (2008) Ro Patent 122:166
26. van Oss CJ, Good RJ, Chaudhury MK (1988) Additive and nonadditive surface tension components and the interpretation of contact angles. Langmuir 4:884–891
27. Rankl M, Laib S, Seeger S (2003) Surface tension properties of surface-coatings for application in biodiagnostics determined by contact angle measurements. Colloid Surf B Biointerface 30:177–186
28. Vijayanand K, Deepak K, Pattanayak DK, Rama Mohan TR, Banerjee R (2005) Interpenetrating blood–biomaterial interactions from surface free energy and work of adhesion. Trends Biomater Artif Organs 18:73–83
29. Kwok SCH, Wang J, Chu PK (2005) Surface energy, wettability, and blood compatibility phosphorus doped diamond-like carbon films. Diamond Relat Mater 14:78–85
30. Agathopoulos S, Nikolopoulos P (1995) Wettability and interfacial interactions in bioceramic-body-liquid systems. J Biomed Mater Res Part A 29:421–429
31. van Oss CJ (1990) Surface properties of fibrinogen and fibrin. J Protein Chem 9:487–491
32. van Oss CJ (2003) Long-range and short-range mechanisms of hydrophobic attraction and hydrophilic repulsion in specific and aspecific interactions. J Mol Recognit 16:177–190
33. Wang KL, Liou WT, Liaw DJ, Huang ST (2008) High glass transition and thermal stability of new pyridine-containing polyimides: effect of protonation on fluorescence. Polymer 49:1538–1546
34. Wang H, Ugomori T, Tanaka K, Kita H, Okamoto KI, Suma Y (2000) Sorption and pervaporation properties of sulfonyl-containing polyimide membrane to aromatic/non-aromatic hydrocarbon mixtures. J Polym Sci Part B Polym Phys 38:2954–2964
35. Gupta K, Yaseen M (1997) Viscosity–temperature relationship of dilute solution of poly(vinyl chloride) in cyclohexanone and in its blends with xylene. J Appl Polym Sci 65:2749–2760
36. Bas C, Tamagna C, Pascal T, Alberola D (2003) On the dynamic mechanical behavior of polyimides based on aromatic and alicyclic dianhydrides. Polym Eng Sci 43:344–355
37. Sader JE, Chon JWM, Mulvaney P (1999) Calibration of rectangular atomic force microscope cantilevers. Rev Sci Instrum 70:3967–3969
38. Sader E, Pacifico J, Green CP, Mulvaney P (2005) General scaling law for stiffness measurement of small bodies with applications to the atomic force microscope. J Appl Phys 97:124903–124909
39. Noy A, Vezenov DV, Lieber CM (1997) Chemical force microscopy. Annu Rev Mater Sci 27:381–421
40. Labarre D (2001) Improving blood-compatibility of polymeric surfaces. Trends Biomater Artif Organs 15:1–3
41. Anderson JM (2001) Biological responses to materials. Annu Rev Mater Res 31:81–110

42. Ioan S, Filimon A (2012) Biocompatibility and antimicrobial activity of some quaternized polysulfones. In: Bobbarala V (ed) Antimicrobial agents, Book 2, Chap 13. InTech, Rijeka, pp 249–274
43. Albu RM, Avram E, Stoica I, Ioanid EG, Popovici D, Ioan S (2011) Surface properties and compatibility with blood of new quaternized polysulfones. J Biomater Nanobiotechol 2:114–123
44. Kawakami H, Takahashi H, Nagaoka S, Nakayama Y (2001) Albumin adsorption to surface of annealed fluorinated polyimide. Polym Adv Technol 12:244–252
45. Nagaoka S, Ashiba K, Kawakami H (2002) Interaction between biocomponents and surface modified fluorinated polyimide. Mater Sci Eng C 20:181–185
46. Reitsma S, Slaaf DW, Vink H, van Zandvoort MAMJ, oude Egbrink MGA (2007) The endothelial glycocalyx: composition, functions, and visualization. Pflugers Arch Eur J Physiol 454:345–359
47. Richardson RR Jr, Miller JA, Reichert WM (1993) Polyimides as biomaterials: preliminary biocompatibility testing. Biomaterials 14:627–635
48. HajjHassan M, Chodavarapu V, Musallam S (2008) NeuroMEMS: neural probe microtechnologies. Sensors 8:6704–6726
49. Ong Y-L, Razatos A, Georgiou G, Sharma MM (1999) Adhesion forces between *E. coli* bacteria and biomaterial surfaces. Langmuir 15:2719–2725
50. Hren J, Polanc S, Kočevar M (2008) The synthesis and transformations of fused bicyclo[2.2.2]octenes. ARKIVOC (Part (i): Special Issue 'Reviews and Accounts), pp 209–231